Hidden similarities in the dynamics of a weakly synchronous marine metapopulation

Tanya L. Rogers[a,1,2] and **Stephan B. Munch**[b]

[a]Marine Science Center, Department of Marine and Environmental Sciences, Northeastern University, Nahant, MA 01908; and [b]Southwest Fisheries Science Center, National Marine Fisheries Service, National Oceanic and Atmospheric Administration, Santa Cruz, CA 95060

Populations of many marine species are only weakly synchronous, despite coupling through larval dispersal and exposure to synchronous environmental drivers. Although this is often attributed to observation noise, factors including local environmental differences, spatially variable dynamics, and chaos might also reduce or eliminate metapopulation synchrony. To differentiate spatially variable dynamics from similar dynamics driven by spatially variable environments, we applied hierarchical delay embedding. A unique output of this approach, the "dynamic correlation," quantifies similarity in intrinsic dynamics of populations, independently of whether their abundance is correlated through time. We applied these methods to 17 populations of blue crab (*Callinectes sapidus*) along the US Atlantic coast and found that their intrinsic dynamics were broadly similar despite largely independent fluctuations in abundance. The weight of evidence suggests that the latitudinal gradient in temperature, filtered through a unimodal response curve, is sufficient to decouple crab populations. As unimodal thermal performance is ubiquitous in ectotherms, we suggest that this may be a general explanation for the weak synchrony observed at large distances in many marine species, although additional studies are needed to test this hypothesis.

synchrony | environmental gradients | time-delay embedding | hierarchical models | *Callinectes sapidus*

Metapopulation synchrony has been studied extensively since the 1990s (1, 2), and the theoretical requirements for synchrony are now well understood. Populations with similar local dynamics will develop correlated fluctuations in abundance if they are coupled by dispersal (3, 4), if they are driven by synchronous environmental fluctuations (the Moran effect; refs. 5 and 6), or if they interact with another species that is synchronized (7–9). In natural populations, synchrony is typically (although not exclusively; see, e.g., ref. 10) inferred from temporal correlations in abundance across subpopulations and the manner in which this correlation decays with distance. The theoretical ingredients for synchrony are supported by laboratory experiments (11, 12), and synchrony has been documented in many natural populations (1).

Importantly, these synchrony-generating mechanisms are generic; they apply to almost any dynamical system. In fact, synchrony theory in the physical sciences is closely parallel (13–15), and shared drivers are routinely used to synchronize independent oscillators in engineering applications (14).

In light of this genericity, when we encounter a pair of populations coupled by dispersal and responsive to highly correlated environmental drivers, we ought to be curious if we observe that they are only weakly correlated. Yet, many marine ectotherms are coupled through panmictic larval dispersal (16) and are strongly responsive to temperature (17, 18), but exhibit only weak correlations among nearby populations, with more distant populations apparently independent (*SI Appendix*, Table S1). Such "weak synchrony" has also been found in insects (19) and birds (20).

Of course, there are many mechanisms which might cause populations to fluctuate independently, and thus asynchrony is typically taken as the null hypothesis (e.g., ref. 21). However, few studies have attempted to differentiate among synchrony-disrupting mechanisms. Here we ask whether heterogeneous fluctuations among populations are due to intrinsic differences in population dynamics or due to similar mechanisms being driven by different local environments.

If we had a well-vetted population model, we might address this question by fitting it to each population using local environmental data and comparing parameter estimates. However, geographic variation in population dynamics (e.g., refs. 22–24) can result from, among other things, latitudinal gradients in growth rate (25), winter survival (26), thermal performance (27), lifespan (28), and community composition (29). Formulating a mechanistic model that can account for spatial variation in vital rates, thermal performance, species interactions, and dispersal is challenging. Yet, our ability to successfully predict population trajectories—and to use these predictions to guide conservation and management actions—depends critically on our understanding of the underlying processes (30). Thus, being able to disentangle differences among dominant mechanisms versus differences in the environmental conditions driving them has important implications for our ability to derive process-based understanding from population time series.

We propose 5 hypotheses for understanding heterogeneous fluctuations in marine metapopulations coupled through larval dispersal. For concreteness, we frame these in terms of a simple model of 2 populations, although the statistical analysis described below does not rely on this model. Population densities x_1 and x_2

Significance

Our ability to predict and manage metapopulations depends on our understanding of their underlying population dynamics. Differences in local dynamics and environmental stochasticity can result in independent population fluctuations but have vastly different implications for population management and predicting how populations will respond to environmental change. Quantifying heterogeneity in local dynamics is particularly challenging because many factors can contribute to differences in local dynamics. Using blue crabs as a case study, we present an approach which can differentiate dissimilar local dynamics from similar local dynamics driven by disparate environmental conditions. This methodology can help us differentiate among mechanisms that decorrelate population trajectories and provide insight into the spatial structure of population dynamics.

ECOLOGY

are driven by the local environment E_1 and E_2, and coupled by dispersal. Specifically,

$$x_{i,t+1} = (1-\mu)F_i(x_{i,t}, E_{i,t}) + \mu F_j(x_{j,t}, E_{j,t})$$

for $i = 1,2$ and $j = 2,1$ where μ is the fraction of the population that disperses each year, and the functions F_1 and F_2 summarize the mechanisms governing population dynamics. In this simple example, there is only one environmental driver, E. If F_1 and F_2 are the same and μ is sufficiently large and/or E_1 and E_2 are strongly correlated, then we expect x_1 and x_2 to be correlated (4, 31).

Obviously, if estimates of x_1 and x_2 are contaminated by sufficient observation noise, populations 1 and 2 will appear uncorrelated (hypothesis I). Less trivially, heterogeneity in dynamics will also reduce synchrony (32–36). Dynamical heterogeneity can emerge from both differences in mechanisms and differences in drivers, so we must distinguish between differences in the shapes of F_1 and F_2 versus differences in the inputs. Thus, weak correlations in abundance can be generated by E_1 and E_2 being uncorrelated (hypothesis II; refs. 31 and 37), F_1 and F_2 being sufficiently different shapes (hypothesis III; refs. 13, 19, and 38), or, if F is nonlinear, differences in the means of E_1 and E_2 (hypothesis IV; refs. 39–41). In what follows, we characterize intrinsic dynamics through the shape of F in order to distinguish this from differences in putative drivers, that is, the inputs to F. Finally, chaotic systems are more difficult to synchronize than stable systems either by coupling or the Moran effect (4, 42–44), so populations may be weakly correlated—even if all other elements are identical—because the local dynamics are chaotic (hypothesis V).

Empirically differentiating among these hypotheses is challenging because several may occur simultaneously. Quantifying heterogeneity in intrinsic dynamics (hypothesis III), as distinct from differences in extrinsic forcing (hypotheses II and IV) presents a particular challenge. For any pair of populations, we want to determine whether F_1 and F_2 are different or whether they are the same but driven by different inputs. Although some insights may be gained by fitting simple parametric models (e.g., refs. 19 and 45–47) and comparing parameter estimates, these methods do not address all of the relevant possibilities. A flexible approach to measuring the hidden similarity in the dynamics (i.e., the shapes of F) of weakly correlated populations is needed.

Here, we used hierarchical Bayesian time-delay embedding models to quantify similarity in intrinsic dynamics and test the relevance of other hypotheses for weak synchrony in metapopulations

(*Materials and Methods* and *SI Appendix*, section 1). Time-delay embedding models are nonparametric time series methods based on Takens' (48) theorem which use time lags to implicitly account for dispersal, species interactions, and other unobserved variables (see, e.g., refs. 49 and 50). The hierarchical Bayesian approach to delay embedding (51, 52) produces a "dynamic correlation" (ρ_D) metric that directly quantifies similarity in the shape of the local maps (i.e., generalized versions of F_1 and F_2) fit to the time series in each pair of locations, allowing us to test for heterogeneity in intrinsic dynamics. When the estimated maps are identical, the dynamic correlation will be close to 1 regardless of the temporal correlation in the time series. Alternatively, if the maps differ between populations, then the dynamic correlation will be reduced (for more details and an illustration, see *SI Appendix*, section 2 and Fig. S1). The fitted models also enable us to evaluate nonlinearity, noise, and the effect of environmental gradients and environmental correlations on predicted metapopulation synchrony. Using these results, combined with traditional analytical methods, we evaluated relative support for the 5 hypotheses.

As a case study, we investigated abundance fluctuations in the blue crab (*Callinectes sapidus*) metapopulation using time series from 17 sites across the US Atlantic coast (Fig. 1*A* and *SI Appendix*, Table S2). Atlantic blue crabs have nearly panmictic larval dispersal (53), and the dynamics of these estuarine ectotherms are known to be strongly influenced by temperature and precipitation (e.g., ref. 54). However, as we document below, populations separated by >200 km are apparently independent, with average correlations indistinguishable from zero.

We first examined metapopulation synchrony by computing correlograms, which express correlation as a function of distance (55), and wavelet coherence plots, which quantify how correlation between population fluctuations varies across different frequencies and over time (56).

We then fit hierarchical delay embedding models to the metapopulation time series data. As predictors, we used 4 lags each of past crab abundance and 3 putative environmental drivers (August sea surface temperature, January air temperature, and Palmer Drought Severity Index [PDSI]), as well as commercial blue crab landings. These were selected based on prior studies and the natural history of the species (*SI Appendix*, section 3 and Table S3). From the delay embedding models, we examined time series predictability, dynamic correlation estimates, and shapes of the population responses to each predictor.
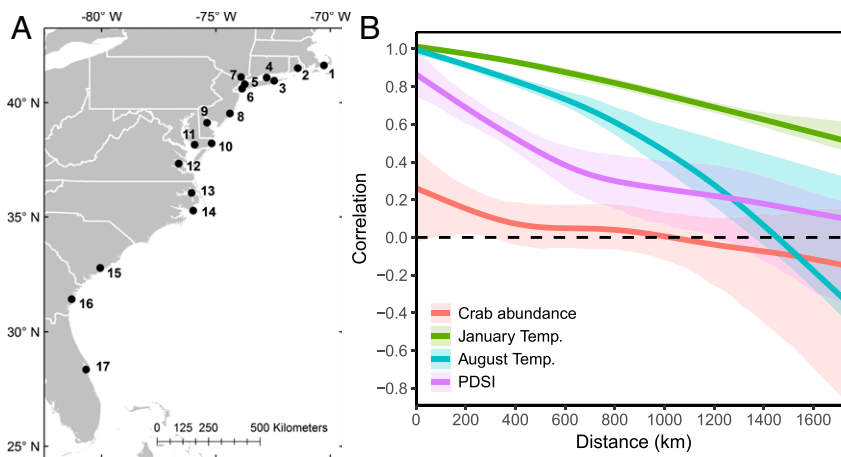

Fig. 1. (*A*) Locations of blue crab populations along the US Atlantic coast that were used in this study. Sources and metadata are provided in *SI Appendix*, Table S2. (*B*) Spline correlograms for crab abundance, January temperature, August temperature, and PDSI. Bands are bootstrapped 95% CIs.
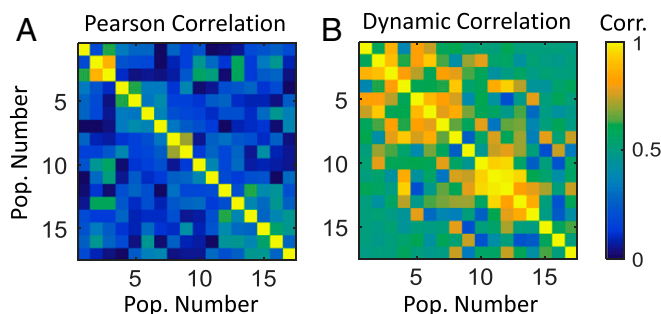
Fig. 2. Pairwise correlation matrices for blue crab populations. (*A*) Pearson correlations (absolute value) for observed crab abundance. (*B*) Dynamic correlations from pairwise hierarchical models.

We then used the fitted models to examine the effects of spatial heterogeneity in intrinsic dynamics and environmental drivers on metapopulation synchrony. To do so, we generated predicted time series under 4 scenarios: 1) without spatial variation in the local dynamics (i.e., all *F*s identical), 2) without spatially variable environmental fluctuations (i.e., all environments perfectly correlated), 3) without environmental gradients (i.e., all means identical), and 4) with neither spatially variable environmental fluctuations nor gradients. We compared the observed and predicted patterns of synchrony using correlograms and the correlation matrix distance (CMD), which measures lack of correspondence between correlation matrices (57).

Results

Pearson correlations among neighboring blue crab populations (<200 km apart) were quite weak (~0.2), and crab populations more than a few hundred kilometers apart were not significantly correlated (Figs. 1*B* and 2*A*). In addition, pairwise wavelet coherence analysis indicated that crab populations displayed irregular and sporadic periods of modest synchrony, with no clear trends or patterns (Dataset S1).

If observation noise renders estimated correlations nonsignificant (hypothesis I), the time series should be effectively unpredictable (58). We examined within-population predictability using independent delay embedding models (i.e., $\rho_D = 0$) and found that crab abundances were fairly predictable, with an average within-sample R^2 of 0.49. Given these estimates and the observed temporal correlation ($\hat{\rho}$), an upper bound on the true (noise-free) temporal correlation between 2 time series (ρ) can be obtained by assuming that all of the residual variance is due to observation error, in which case $\rho_{ij} \approx \hat{\rho}_{ij}/(R_i^2 R_j^2)^{1/2}$ (*SI Appendix,* section 4). Using this upper bound, correlations increased among nearby sites, but the distance over which populations became uncorrelated was still quite short (<400 km) (*SI Appendix,* Fig. S2*B*).

Theory on the Moran effect predicts that the distance over which populations are correlated should be at least half that of the environmental drivers (hypothesis II; refs. 31 and 59). However, the putative drivers (temperature, precipitation) remained highly correlated at distances of 1,400 km or more, several times longer than the spatial scale for blue crabs (Fig. 1*B* and *SI Appendix,* Fig. S3). Of course, this can't rule out the possibility that there are other drivers with shorter spatial scales.

Since heterogeneity in intrinsic dynamics can produce uncorrelated fluctuations (hypothesis III), we next evaluated dynamical similarity across pairs of sites. Dynamic correlations (ρ_D) indicated the local maps were quite similar among sites (0.59 on average; Fig. 2*B*), with nearby populations having slightly higher ρ_D values. A reduced model that omitted environmental drivers also resulted in high ρ_D values (*SI Appendix,* Fig. S2*I*).

Our next step was to fit a single hierarchical model for all populations, hereafter the "full model," using pairwise ρ_D values taken from the matrix in Fig. 2*B* and use this model to evaluate the effects of each input. Conditional responses to each predictor (with other inputs fixed at their mean) were similar across locations and exhibited fairly smooth latitudinal gradients (Fig. 3). The predictor with the largest effect was crab population size the previous year ($t − 1$). At $t − 1$, the effects of January and August temperature were unimodal or increasing, with higher temperatures predicting higher crab abundance. In contrast, for January temperature at $t − 2$ and August temperature at $t − 2$ and $t − 3$, higher temperatures predicted lower crab abundance. The effects of population size and temperature were nonadditive (Fig. 4). PDSI, landings, and all inputs at lag $t − 4$ had negligible effects (see *SI Appendix,* Fig. S4 for all plots). Correlations among the model residuals were not significantly different from zero at all spatial distances, suggesting that the major drivers have been accounted for.

We used the fitted model to predict patterns of synchrony under different scenarios to further test the hypotheses. All predictions used step-ahead forecasts based on leave-one-out cross-validation. First, we generated predictions from the full model using the observed values of all predictors (see *SI Appendix,* Fig. S6 for plots of observed and predicted time series). Correlations among the predicted values resembled those of the observed values (Table 1 and *SI Appendix,* Fig. S2*D*). They were slightly higher within 200 km (averaging around 0.4 as opposed to 0.2; Fig. 5*A*), but the distance at which populations became uncorrelated was similar.

To further explore the importance of local dynamics, we made predictions using identical maps for all populations (i.e., $\rho_D = 1$). The difference in predicted synchrony between this and the full model reflects the contribution of local differences in intrinsic dynamics (hypothesis III). We found that the predictions with identical dynamics had slightly higher correlations (~0.45 within 200 km) which decayed to zero over a slightly larger distance (~500 km vs. 300 km) (Table 1, Fig. 5*A*, and *SI Appendix,* Fig. S2*C*).

Environmental drivers, particularly temperature, displayed a strong latitudinal gradient, despite their annual fluctuations being highly synchronous (*SI Appendix,* Figs. S7*A* and S8). So we next compared the effects of environmental variability (hypothesis II) and environmental gradients (hypothesis IV) on predicted synchrony (Table 1, Fig. 5*B*, and *SI Appendix,* Figs. S2 *D–G* and S7).
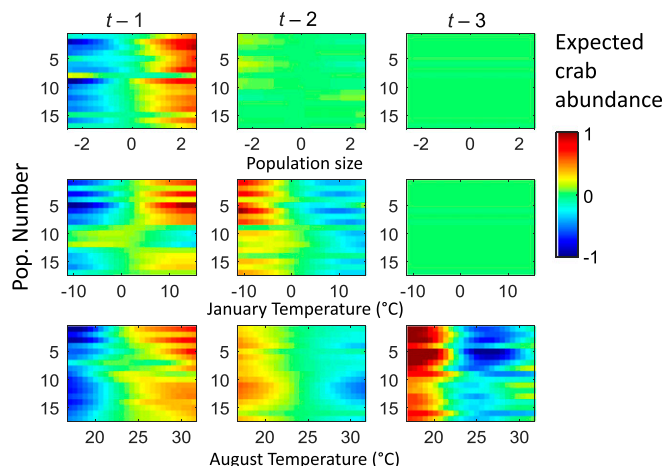

Fig. 3. Conditional responses of crab populations to 3 lags of 3 predictor variables from the hierarchical model with pairwise ρ_D values. Expected crab abundance (scaled to mean 0) at time *t* is evaluated over each predictor variable for each population, holding all other predictors fixed at their mean value. Results for all predictor variables are shown in *SI Appendix,* Fig. S4.
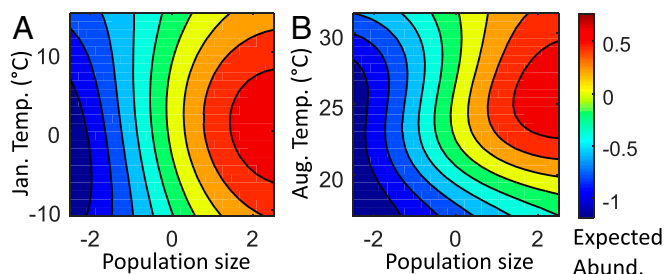
ECOLOGY

Fig. 4. Conditional responses of crab populations to population size and (*A*) January temperature and (*B*) August temperature at lag *t* – 1 for population 9 (results for all populations are shown in *SI Appendix*, Fig. S5). Expected crab abundance at time *t* is evaluated while holding all other predictors fixed at their mean value.

Removing differences in local variability (environments perfectly correlated but retaining local means) did not change predicted synchrony. In contrast, removing the differences in local means but retaining temporal variability greatly increased the distance over which populations were positively correlated (>1,000 km). Removing differences in both local mean and variability further increased the distance over which populations were correlated. Thus it appears that heterogeneity in mean environmental conditions, rather than in environmental fluctuations, per se, is required to produce weak synchrony in blue crabs.

Finally, because chaotic dynamics are more difficult to synchronize than stable dynamics (hypothesis V), we estimated the dominant Lyapunov exponent for each population using the method of Rosenstein et al. (60). The Lyapunov exponent quantifies the mean rate of trajectory divergence, and positive values are typically interpreted as indicia of chaos (see, e.g., refs. 61 and 62). Lyapunov exponents were all positive and similar in magnitude (mean, 0.1; SD, 0.02; Fig. 6 and *SI Appendix*, section 5).

Discussion

Panmictic larval dispersal and highly correlated environmental drivers originally lead us to anticipate that blue crabs would be synchronous across much of their range; however, populations were largely uncorrelated across the 1,700-km range we examined. While all of the hypotheses we explored likely play some role, the strongest evidence suggests that intrinsic local dynamics are broadly similar and that the latitudinal gradient in temperature, filtered through nonlinear thermal response curves (hypothesis IV), acts to disrupt synchrony in the blue crab metapopulation.

We initially suspected the crab populations were, in fact, correlated but that low-quality data rendered this undetectable. However, if observation noise were the main culprit, model R^2 would be low, and the upper bound on the correlations obtained by attributing all residual variation to observation noise would have been high. Since this was not the case, something more interesting must be going on.

We next hypothesized that heterogeneity in abundance fluctuations stems from heterogeneity in intrinsic dynamics. This seemed reasonable, since current management for Atlantic blue crabs is based on models fit separately for each state or estuary. Differences in intrinsic dynamics could result from geographic variation in crab life histories, thermal performance, or the species with which the crabs interact (29). However, high values for ρ_D from the hierarchical delay embedding model revealed that the dynamics in different locations are quite similar. Forcing all populations to have identical dynamics ($\rho_D = 1$) did not substantially reduce model fit or increase synchrony among predictions. Hence, the largely uncorrelated fluctuations of the crab populations belie consistent responses to past abundances and environmental conditions.

In contrast, differences in mean environmental conditions and nonlinear responses to those conditions appear to play an important role. Estimated responses to temperature were strongly nonlinear (Fig. 3) and interacted with population size (Fig. 4). Population growth rates increased with population size and exhibited a unimodal or increasing response to temperature at lag *t* – 1. This is consistent with studies on blue crab physiology (63). The effect of temperature at lag *t* – 2 was inverted and requires further consideration. Rather than a delayed effect of crab physiology, we suspect this represents a temperature-mediated interaction with another species. For instance, if the abundance of a predator is positively influenced by temperature, this would appear as a negative response of crabs to past temperatures. Temperature was correlated over distances too long to explain weak synchrony in blue crabs (31, 45, 59). However, differences in mean temperature, filtered through a unimodal response curve, cause the net effect of temperature fluctuations to differ, which could decouple abundance fluctuations. Similar arguments have been made for why populations near or far from thermal tolerance limits will have different responses to climate change (64). Most importantly, removing the environmental gradient from predictions resulted in long-distance synchrony (Fig. 5*B*), providing strong support for this mechanism. Forcing populations with perfectly correlated environmental fluctuations did not markedly increase synchrony.

The fact that the Lyapunov exponent estimates were positive is also consistent with the idea that populations diverge because of nonlinear dynamics interacting with differences in the local environment. Although suggestive of chaos, positive estimates for Lyapunov exponents may also be generated by process noise, and we cannot definitively differentiate between them. However, an analogous result was found in an intertidal community where trajectory divergence was driven by seasonal, as opposed to spatial, differences in environmental conditions (62).

The Atlantic coast of North America exhibits one of the steepest coastal temperature gradients in the world. However, the slope of the gradient in mean annual temperature has decreased by 10% over the last 30 y, due to warming at high latitudes (65), and the gradient in August temperature has declined by 25% over the last 20 y in our study region. Our results suggest that there is some chance that blue crab populations will become more synchronized as this gradient weakens—a source of some concern given the importance of weak synchrony for maintaining portfolio effects (66, 67). However, the presence of even moderate gradients may be sufficient; reducing the environmental gradient by 25% did not significantly increase predicted synchrony among crab populations (*SI Appendix*, Fig. S9). This is perhaps encouraging, although warming will have many other adverse effects (17).

Although we have studied only a single species, the mechanism we identified is likely to be quite common. Unimodal responses to temperature are ubiquitous among ectotherms (68), which implies that a small increase in temperature will increase population growth in regions where the mean is low and decrease growth where the mean is high. Highly correlated fluctuations in temperature, superimposed upon a latitudinal cline in

Table 1. CMDs between observed and predicted correlations generated under different scenarios

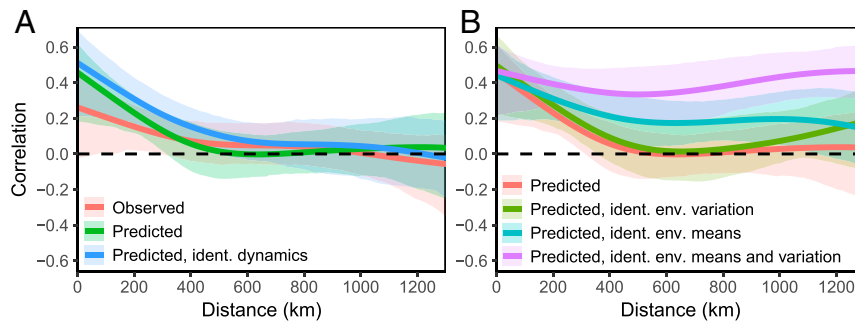| Model predictions made using	CMD
Observed values	0.308
Identical dynamics	0.336
Identical environmental variation	0.376
Identical environmental means	0.537
Identical environmental means and variation	0.702

Rogers and Munch

Fig. 5. Spline correlograms for out-of-sample predictions generated under different scenarios. (*A*) Correlograms for observed data and for predictions from the hierarchical model with either pairwise ρ_D values or ρ_D fixed to 1 (identical [ident.] dynamics). Predictions were made over the observed environmental conditions. (*B*) Correlograms for predictions from the hierarchical model with pairwise ρ_D values, using either the observed environmental (env.) conditions, or fixing the environmental variation or means to be identical across sites. Bands are bootstrapped 95% CIs.

the mean, will therefore have opposing effects on populations at high and low latitudes, leading to uncorrelated fluctuations in abundance. Further study is needed to determine whether weak correlations in abundance observed in other ectotherms can be understood similarly. This mechanism has been proposed to explain reduced synchrony in insects across elevational temperature gradients, although responses to temperature were not directly quantified (41).

A prevailing problem in the study of ecological dynamics is that many different processes can produce similar patterns. The path from pattern to process has historically involved an interplay of experiments and theory (e.g., refs. 69 and 70). But, for large ecosystems, manipulative experiments can be infeasible, and we must attempt to understand process by fitting models to data. We argue that robust inferences about putative mechanisms require tools that are unencumbered by assumptions about other aspects of the dynamics. We suggest that continued development and application of equation-free approaches (e.g., refs. 71 and 72) will be valuable in pursuing a mechanistic understanding of complex ecosystems as well as constructing robust approaches to conservation and management (e.g., ref. 73).

Materials and Methods

Blue Crabs. Blue crabs are commercially important crustaceans found in coastal estuaries. In the United States, they are found from Massachusetts to the Gulf of Mexico. They mature in 1 to 2 y and have a typical lifespan of 2 to 3 y. The relatively short generation time of blue crabs and the availability of long-term monitoring data over a large spatial scale make blue crabs an ideal case study. More information about blue crabs and their life cycle is provided in *SI Appendix*, section 3.

We compiled long-term (19 to 57 y) time series data on blue crab abundance (mean annual catch per unit effort) for 17 populations sampled in fishery-independent surveys in estuaries across the US Atlantic coast (Fig. 1*A* and *SI Appendix*, Table S2). Although the survey methods employed differ across populations, they have remained consistent through time within each survey, and provide an index of local density. To remove scale differences across sites resulting from differences in gear efficiency, each population time series was rescaled by the within-site mean and natural log-transformed. Other standardization procedures (e.g., subtracting mean and dividing by SD) produced similar results. Environmental predictors were centered on 0 across sites and rescaled to a global variance of 1. For a detailed description and justification of the predictor variables used, see *SI Appendix*, section 3.

Gaussian Process Time-Delay Embedding. Takens' theorem (48) and its extension to nonautonomous systems (74) justifies modeling the abundance from a single site i as a function of its lags, $y_{i,t-1}, \ldots y_{i,t-L}$, and relevant external drivers, $E_{i,t-1}, \ldots E_{i,t-L}$. That is, $y_{i,t} = f_i(\mathbf{x}_{i,t}) + \varepsilon_{i,t}$ with $\mathbf{x}_{i,t} = \{y_{i,t-1}, \ldots y_{i,t-L}, E_{i,t-1}, \ldots E_{i,t-L}\}$. In practice, the mapping is not perfect; hence the model includes approximation error or process uncertainty, $\varepsilon_{i,t} \sim N(0, V_\varepsilon)$. The functional form for $f_i(\mathbf{x}_{i,t})$ is not known a priori and is determined empirically, allowing for arbitrary interactions among the predictors. We estimate the shape of the nonlinear functions f_i

using Bayesian Gaussian process (GP) regression (52, 75). Further details of the GP model implementation are provided in *SI Appendix*, section 1. For a complete description of the model, see Munch et al. (52).

To integrate information from multiple sites, we use a hierarchical model structure. Specifically, we decompose the site-specific delay-coordinate map, f_i into shared, μ, and independent, g_i, components, $f_i = \mu + g_i$ where $\mu \sim GP(0, C)$ and $g_i \sim GP(0, \Sigma)$. The total point-wise prior variance in f_i is partitioned into within- and across-site components, given by $\varpi^2 = \tau^2 + \sigma^2$. We write $\sigma^2 = \rho_D \varpi^2$ and $\tau^2 = (1 - \rho_D)\varpi^2$ with ρ_D between 0 and 1. Under this specification, the correlation between 2 site-specific maps evaluated at the same input, $f_i(x)$ and $f_j(x)$, reduces to ρ_D. Moreover, simulations indicate that ρ_D provides a good approximation of $\langle f_i, f_j \rangle / [\langle f_i, f_i \rangle \langle f_j, f_j \rangle]^{1/2}$ where $\langle f_i, f_j \rangle = \int f_i(\mathbf{x})f_j(\mathbf{x})dx$ and the integral covers domain of the data (51). Thus ρ_D (the "dynamic correlation") indicates the similarity of the reconstructed maps between sites. The fs are identical when $\rho_D = 1$ and independent when $\rho_D = 0$.

Conditional on the data and the maximum a posteriori estimates of the parameters, the posterior for f is $GP(m_c, \Sigma_c)$, where m_c and Σ_c are the posterior mean and covariance functions obtained using standard formulae for conditioning in multivariate normals (75).

We used the fitted GP model to generate out-of-sample predictions under different environmental scenarios as additional tests for hypotheses II and IV. Specifically, we evaluated the contribution of locally distinct means and locally distinct temporal fluctuations to synchrony reduction. This resulted in 4 combinations of prediction scenarios: 1) no gradient, identical fluctuations; 2) no gradient, original fluctuations; 3) original gradient, identical fluctuations; and 4) original gradient, original fluctuations (*SI Appendix*, Fig. S7). The CMD used to compare observed and predicted correlation matrices is defined as 1 minus the Pearson correlation between the off-diagonal elements (57) and is analogous to a likelihood ratio test for different correlation structures when the means are identical.

Data and Software Availability. All analyses were performed in Matlab, with the exception of the correlograms and pairwise wavelet coherence analyses, which were conducted using the packages "ncf" (76) and "biwavelet" (77), respectively, in R v.3.3.1. The analysis code may be obtained from the authors upon request. The crab and environmental data were obtained from the sources listed in *SI Appendix*, Tables S2 and S3.
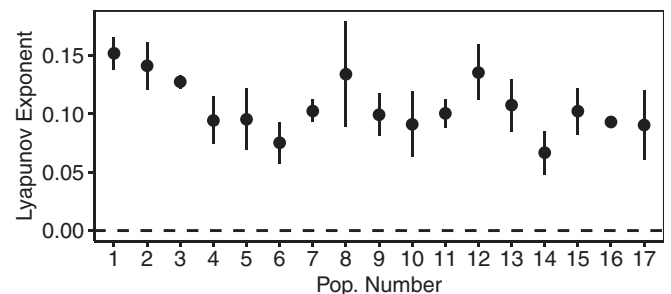

Fig. 6. Estimates of the dominant Lyapunov exponent for blue crab populations. Error bars are 95% CIs.

1. A. Liebhold, W. D. Koenig, O. N. Bjørnstad, Spatial synchrony in population dynamics. *Annu. Rev. Ecol. Evol. Syst.* **35**, 467–490 (2004).
2. O. N. Bjørnstad, R. A. Ims, X. Lambin, Spatial population dynamics: Analyzing patterns and processes of population synchrony. *Trends Ecol. Evol.* **14**, 427–432 (1999).
3. J. Molofsky, Population dynamics and pattern formation in theoretical populations. *Ecology* **75**, 30–39 (1994).
4. E. Ranta, V. Kaitala, P. Lundberg, Population variability in space and time: The dynamics of synchronous population fluctuations. *Oikos* **83**, 376–382 (1998).
5. P. A. P. Moran, The statistical analysis of the Canadian Lynx cycle: II. Synchronization and meteorology. *Aust. J. Zool.* **1**, 291–298 (1953).
6. E. Ranta, V. Kaitala, J. Lindström, E. Helle, J. Lindstrom, The Moran effect and synchrony in population dynamics. *Oikos* **78**, 136 (1997).
7. B. Blasius, A. Huppert, L. Stone, Complex dynamics and phase synchronization in spatially extended ecological systems. *Nature* **399**, 354–359 (1999).
8. B. Cazelles, G. Boudjema, The Moran effect and phase synchronization in complex spatial community dynamics. *Am. Nat.* **157**, 670–676 (2001).
9. R. A. Ims, H. Steen, Geographical synchrony in microtine population cycles: A theoretical evaluation of the role of nomadic avian predators. *Oikos* **57**, 381 (1990).
10. L. W. Sheppard, J. R. Bell, R. Harrington, D. C. Reuman, Changes in large-scale climate alter spatial synchrony of aphid pests. *Nat. Clim. Chang.* **6**, 610–613 (2016).
11. J. W. Fox, D. A. Vasseur, S. Hausch, J. Roberts, Phase locking, the Moran effect and distance decay of synchrony: Experimental tests in a model system. *Ecol. Lett.* **14**, 163–168 (2011).
12. C. Fontaine, A. Gonzalez, Population synchrony induced by resource fluctuations and dispersal in an aquatic microcosm. *Ecology* **86**, 1463–1471 (2005).
13. Y. Kuramoto, "Self-entrainment of a population of coupled non-linear oscillators" in International Symposium on Mathematical Problems in Theoretical Physics, H. Araki, Ed. (Springer, Berlin, Germany, 1975), pp. 420–422.
14. A. Pikovsky, M. Rosenblum, J. Kurths, *Synchronization: A Universal Concept in Nonlinear Sciences* (Cambridge University Press, 2001).
15. K. Kaneko, Overview of coupled map lattices. *Chaos* **2**, 279–282 (1992).
16. R. K. Cowen, S. Sponaugle, Larval dispersal and marine population connectivity. *Annu. Rev. Mar. Sci.* **1**, 443–466 (2009).
17. C. D. G. Harley et al., The impacts of climate change in coastal marine systems. *Ecol. Lett.* **9**, 228–241 (2006).
18. S. M. Lucey, J. A. Nye, Shifting species assemblages in the Northeast US Continental Shelf Large Marine Ecosystem. *Mar. Ecol. Prog. Ser.* **415**, 23–33 (2010).
19. M. Peltonen, A. M. Liebhold, O. N. Bjørnstad, D. W. Williams, Spatial synchrony in forest insect outbreaks: Roles of regional stochasticity and dispersal. *Ecology* **83**, 3120–3129 (2002).
20. W. D. Koenig, Spatial autocorrelation and local disappearances in wintering North American birds. *Ecology* **82**, 2636–2644 (2001).
21. M. M. Stachura et al., Linking Northeast Pacific recruitment synchrony to environmental variability. *Fish. Oceanogr.* **23**, 389–408 (2014).
22. O. N. Bjørnstad, W. Falck, N. C. Stenseth, A geographic gradient in small rodent density fluctuations: A statistical modelling approach. *Proc. Biol. Sci.* **262**, 127–133 (1995).
23. D. W. Williams, A. M. Liebhold, Spatial scale and the detection of density dependence in spruce budworm outbreaks in eastern North America. *Oecologia* **124**, 544–552 (2000).
24. P. Turchin, I. Hanski, An empirically based model for latitudinal gradient in vole population dynamics. *Am. Nat.* **149**, 842–874 (1997).
25. D. O. Conover, T. M. C. Present, Countergradient variation in growth rate: Compensation for length of the growing season among Atlantic silversides from different latitudes. *Oecologia* **83**, 316–324 (1990).
26. S. B. Munch, M. Mangel, D. O. Conover, Quantifying natural selection on body size from field data: Winter mortality in *Menidia menidia*. *Ecology* **84**, 2168–2177 (2003).
27. B. J. Sinclair, C. M. Williams, J. S. Terblanche, Variation in thermal performance among insect populations. *Physiol. Biochem. Zool.* **85**, 594–606 (2012).
28. S. B. Munch, S. Salinas, Latitudinal variation in lifespan within species is explained by the metabolic theory of ecology. *Proc. Natl. Acad. Sci. U.S.A.* **106**, 13860–13864 (2009).
29. V. D. Engle, J. K. Summers, Latitudinal gradients in benthic community composition in Western Atlantic estuaries. *J. Biogeogr.* **26**, 1007–1023 (1999).
30. K. Cuddington et al., Process-based models are required to manage ecological systems in a changing world. *Ecosphere* **4**, 20 (2013).
31. R. Lande, S. Engen, B. E. Sæther, Spatial scale of population synchrony: Environmental correlation versus dispersal and density regulation. *Am. Nat.* **154**, 271–281 (1999).
32. S. Engen, R. Lande, B.-E. Sæther, Migration and spatiotemporal variation in population dynamics in a heterogeneous environment. *Ecology* **83**, 570–579 (2002).
33. E. E. Goldwyn, A. Hastings, Small heterogeneity has large effects on synchronization of ecological oscillators. *Bull. Math. Biol.* **71**, 130–144 (2009).
34. B. Hugueny, Spatial synchrony in population fluctuations: Extending the Moran theorem to cope with spatially heterogeneous dynamics. *Oikos* **115**, 3–14 (2006).
35. A. M. Liebhold, D. M. Johnson, O. N. Bjørnstad, Geographic variation in density-dependent dynamics impacts the synchronizing effect of dispersal and regional stochasticity. *Popul. Ecol.* **48**, 131–138 (2006).
36. J. A. Walter et al., The geography of spatial synchrony. *Ecol. Lett.* **20**, 801–814 (2017).
37. L. M. Pecora, T. L. Carroll, Synchronization of chaotic systems. *Chaos* **25**, 097611 (2015).
38. B. J. Swanson, D. R. Johnson, Distinguishing causes of intraspecific synchrony in population dynamics. *Oikos* **86**, 265–274 (1999).
39. B. E. Saether et al., Geographical gradients in the population dynamics of North American prairie ducks. *J. Anim. Ecol.* **77**, 869–882 (2008).
40. N. C. Stenseth et al., Common dynamic structure of Canada lynx populations within three climatic regions. *Science* **285**, 1071–1073 (1999).
41. S. B. Hagen, J. U. Jepsen, N. G. Yoccoz, R. A. Ims, Anisotropic patterned population synchrony in climatic gradients indicates nonlinear climatic forcing. *Proc. Biol. Sci.* **275**, 1509–1515 (2008).
42. D. A. Vasseur, J. W. Fox, Phase-locking and environmental fluctuations generate synchrony in a predator-prey community. *Nature* **460**, 1007–1010 (2009).
43. L. Becks, H. Arndt, Different types of synchrony in chaotic and cyclic communities. *Nat. Commun.* **4**, 1359 (2013).
44. J. C. Allen, W. M. Schaffer, D. Rosko, Chaos reduces species extinction by amplifying local population noise. *Nature* **364**, 229–232 (1993).
45. J. Roughgarden, A simple model for population dynamics in stochastic environments. *Am. Nat.* **109**, 713–736 (1975).
46. S. Engen, R. Lande, B. E. Seæther, T. Bregnballe, Estimating the pattern of synchrony in fluctuating populations. *J. Anim. Ecol.* **74**, 601–611 (2005).
47. B. E. Saether et al., The extended Moran effect and large-scale synchronous fluctuations in the size of great tit and blue tit populations. *J. Anim. Ecol.* **76**, 315–325 (2007).
48. F. Takens, "Detecting strange attractors in turbulence" in *Dynamical Systems and Turbulence*, D. A. Rand, L. S. Young, Eds. (Springer, New York, 1981), pp. 366–381.
49. G. Sugihara, R. M. May, Nonlinear forecasting as a way of distinguishing chaos from measurement error in time series. *Nature* **344**, 734–741 (1990).
50. S. B. Munch, A. Brias, G. Sugihara, T. L. Rogers, Frequently asked questions about nonlinear dynamics and empirical dynamic modelling. *ICES J. Mar. Sci.* 10.1093/icesjms/fsz209 (2019).
51. V. Poynor, S. Munch, Combining functional data with hierarchical Gaussian process models. *Environ. Ecol. Stat.* **24**, 175–199 (2017).
52. S. B. Munch, V. Poynor, J. L. Arriaza, Circumventing structural uncertainty: A Bayesian perspective on nonlinear forecasting for ecology. *Ecol. Complex.* **32**, 134–143 (2017).
53. A. L. McMillen-Jackson, T. M. Bert, P. Steele, Population genetics of the blue crab *Callinectes sapidus*: Modest population structuring in a background of high gene flow. *Mar. Biol.* **118**, 53–65 (1994).
54. M. S. Rome, A. C. Young-Williams, G. R. Davis, A. H. Hines, Linking temperature and salinity tolerance to winter mortality of Chesapeake Bay blue crabs (*Callinectes sapidus*). *J. Exp. Mar. Biol. Ecol.* **319**, 129–145 (2005).
55. O. N. Bjørnstad, W. Falck, Nonparametric spatial covariance functions: Estimation and testing. *Environ. Ecol. Stat.* **8**, 53–70 (2001).
56. B. Cazelles et al., Wavelet analysis of ecological time series. *Oecologia* **156**, 287–304 (2008).
57. M. Herdin, N. Czink, H. Ozcelik, E. Bonek, "Correlation matrix distance, a meaningful measure for evaluation of non-stationary MIMO channels" in *2005 IEEE 61st Vehicular Technology Conference* (Institute of Electrical and Electronics Engineers, 2005), vol. 1, pp. 136–140.
58. T. Rouyer et al., Complex interplays among population dynamics, environmental forcing, and exploitation in fisheries. *Proc. Natl. Acad. Sci. U.S.A.* **105**, 5420–5425 (2008).
59. S. Engen, Spatial synchrony and harvesting in fluctuating populations: Relaxing the small noise assumption. *Theor. Popul. Biol.* **116**, 18–26 (2017).
60. M. T. Rosenstein, J. J. Collins, C. J. De Luca, A practical method for calculating largest Lyapunov exponents from small data sets. *Physica D Nonlinear Phenom.* **65**, 117–134 (1993).
61. S. P. Ellner, P. Turchin, Chaos in a noisy world: New methods and evidence from time-series analysis. *Am. Nat.* **145**, 343–375 (1995).
62. E. Benincà, B. Ballantine, S. P. Ellner, J. Huisman, Species fluctuations sustained by a cyclic succession at the edge of chaos. *Proc. Natl. Acad. Sci. U.S.A.* **112**, 6389–6394 (2015).
63. J. S. Holland, D. V. Aldrich, K. Strawn, Effects of temperature and salinity on growth, food conversion, survival and temperature resistance of juvenile blue crabs, *Callinectes sapidus* Rathbun (Sea Grant Publ. TAMU-SG-71-222, National Oceanic and Atmospheric Administration, 1971).
64. J. M. Sunday, A. E. Bates, N. K. Dulvy, Thermal tolerance and the global redistribution of animals. *Nat. Clim. Chang.* **2**, 686–690 (2012).
65. H. Baumann, O. Doherty, Decadal changes in the world's coastal latitudinal temperature gradients. *PLoS One* **8**, e67596 (2013).

66. D. E. Schindler et al., Population diversity and the portfolio effect in an exploited species. *Nature* **465**, 609–612 (2010).
67. L. Yamane, L. W. Botsford, D. P. Kilduff, Tracking restoration of population diversity via the portfolio effect. *J. Appl. Ecol.* **55**, 472–481 (2018).
68. R. B. Huey, J. G. Kingsolver, Evolution of thermal sensitivity of ectotherm performance. *Trends Ecol. Evol.* **4**, 131–135 (1989).
69. G. F. Gause, Experimental analysis of Vito Volterra's mathematical theory of the struggle for existence. *Science* **79**, 16–17 (1934).
70. R. T. Paine, Food web complexity and species diversity. *Am. Nat.* **100**, 65–75 (1966).
71. E. R. Deyle, R. M. May, S. B. Munch, G. Sugihara, Tracking and forecasting ecosystem interactions in real time. *Proc. R Soc. B Biol. Sci.* **283**, 20152258 (2016).
72. G. Sugihara et al., Detecting causality in complex ecosystems. *Science* **338**, 496–500 (2012).
73. C. Boettiger, M. Mangel, S. Munch, Avoiding tipping points in fisheries management through Gaussian process dynamic programming. *Proc. R Soc. B Biol. Sci.* **282**, 20141631 (2015).
74. J. Stark, Delay embeddings for forced systems. I. Deterministic forcing. *J. Nonlinear Sci.* **9**, 255–332 (1999).
75. E. Rasmussen, K. I. Williams, *Gaussian Processes for Machine Learning* (MIT Press, 2006).
76. O. N. Bjornstad, ncf: Spatial Nonparametric Covariance Functions (R package version 1.1-7, 2016). https://cran.r-project.org/web/packages/ncf/index.html.
77. T. C. Gouhier, A. Grinsted, V. Simko, R package "biwavelet": Conduct Univariate and Bivariate Wavelet Analyses, Version 0.20.15. https://github.com/tgouhier/biwavelet. Accessed 9 April 2018.

ECOLOGY

Rogers and Munch